Research Article Open Access

Joshi Laxmikanth Rao*, Kotamarthi Bhanuprakash

Push-pull effect on the geometrical, optical and charge transfer properties of disubstituted derivatives of *mer*-tris(4-hydroxy-1,5-naphthyridinato) aluminum (*mer*-AlND3)

DOI: 10.1515/chem-2016-0001 received April 23, 2015; accepted November 14, 2015.

Abstract: To design innovative and novel optical materials with high mobility, two kinds of disubstituted derivatives for *mer*-tris(4-hydroxy-1,5-naphthyridinato) aluminum (mer-AlND3) with push (EDG)-pull (EWG) substituents have been designed. The structures of mer-tris(8-EDG-2-EWG-4-hydroxy-1,5-naphthyridinato) aluminum mer-tris(8-EWG-2-EDG-4-hydroxy-1,5and naphthyridinato) aluminum (type II) in the ground and first excited states have been optimized at the B3LYP/6-31G(D) and CIS/6-31G(D) level of theory, respectively. It can be seen from frontier molecular orbitals analysis, in all these complexes, the highest occupied molecular orbital (HOMO) is localized on the pyridine-4-ol ring of A-ligand while lowest unoccupied molecular orbital (LUMO) is on the pyridyl ring of B-ligand in ground state irrespective of electron donor/acceptor substitution present on the ligands similar to that of mer-tris(8hydroxyguinoline) aluminum (mer-Alg3) and parent mer-AlND3. The absorption and emission wavelengths have been evaluated at the TD-PBEO/6-31G(D) level and it can be see that all the type I derivatives show blue shift while most of the type II derivatives show red shift compared to mer-AlND3. All the disubstituted complexes have showed hypsochromic shifts in both the absorption and emission spectra when compared with the calculated absorption and emission spectra respectively of *mer*-Alq3. It can be seen that the reorganization energies of some of the disubstituted derivatives are comparable with merAlq3 and these derivatives might be good candidates for emitting materials in OLED.

Keywords: OLED, DFT, Optical properties, Charge transfer, *mer*-AlND3

1 Introduction

Organic light-emitting diodes (OLED) are currently gaining importance as a promising technology for the fabrication of flat-panel display devices [1-7]. OLEDs are heterojunction devices in which layers of organic transport materials are usually incorporated into devices as amorphous thin solid films [8]. Organometallic complexes are suitable candidates for OLEDs [9-18] due to their stability, emission-color purity, and availability both as singlet [19] and triple emitters [20] and their ease of deposition by means of thermal vacuum evaporation. Following the initial report of utilization of mer-Alq3 as electron transport material and emitting layer in OLED [21,22], the derivatives of metal quinolates has become the focus of new electroluminescent materials research with mer-Alq3 being the most often used [8,23,24]. Although research into the development of OLEDs in the past decade is rapidly growing, in recent years the studies of the fundamental molecular properties of metaloguinolates have been reported in the literature [25-39]. It is clear from these reports that a detailed understanding of the relationship between the ligand structure and optical properties of the resulting Al-complex is essential to make progress in the improvement of OLED devices. The optical properties of mer-Alg3 -type derivatives are dominated by the ligand centered excited states [37], which originate from the electronic π - π * transitions in the quinolinolate ligands [38] and HOMO and LUMO orbitals are located on the phenoxide side of the ligand and on the pyridyl side

Chemical Technology Hyderabad- 500 007, Telangana, India

^{*}Corresponding author: Joshi Laxmikanth Rao: I & PC Division, CSIR-Indian Institute of Chemical Technology Hyderabad- 500 007, Telangana, India, E-mail: lkjoshiji@yahoo.com Kotamarthi Bhanuprakash: I & PC Division, CSIR-Indian Institute of

of the ligand respectively [40-42]. This indicates that the substituent attached to the quinolinolate ligand plays an important role in tuning the emission of the Al-complex.In general electron donating groups attached to pyridine ring cause a blue shift in the emission while the introduction to phenoxide ring cause a red shift [43-48]. The electron withdrawing groups such as chloro [39] and cyano [16] show almost negligible emission shifts, while the strong electron withdrawing group such as sulfonamide results in blue shifted emission [50] and the substitution of fluorine at different positions in mer-Alg3 ligand show variable emission [51]. The mer-AlND3 and its methyl derivatives are reported to be the blue version analogues of mer-Alg3 and can be used as electron transporting layer as well as emitting layer in the OLEDs [52]. So in the present study our main aim is to design theoretically some new novel emitting materials with tunable color as well as high charge mobility by introducing electron donating groups (EDG) and electron withdrawing groups (EWG) at 8 and 2 positions and vice versa on 4-hydroxy-1,5-naphthyridinato ligands respectively in *mer*-AlND3. The present work deals with the detailed theoretical study of these Al-complexes for their structural, optical and charge transport properties on two types of disubstituted derivatives of mer-AlND3 with push (EDG)-pull (EWG) substituents (where EDG = -CH3/-NH2 and EWG = -CN/-C1). For the type I, disubstituted derivatives (1-4), the mer-tris(8-EDG-2-EWG-4-hydroxy-1,5-naphthyridinato) aluminum depict for EDG on position 8 and EWG group on position 2 on 4-hydroxy-1,5-naphthyridinato ligands, where as for type II (5-8), the *mer*-tris(8-EWG-2-EDG-4-hydroxy-1,5-naphthyridinato) aluminum represent for EDG on position 2 and EWG on position 8 on 4-hydroxy-1,5-naphthyridinato ligands. The ab initio (HF) and DFT (B3LYP) methods have been used to optimize the ground-state geometries. The first singlet excited-state geometries have been optimized at the ab *initio* configuration interaction singles (CIS) level of theory. The excited-state geometry has been compared with the optimized ground state structure. The time-dependent density functional theory (TD-DFT) methods have been used to calculate the absorption and the emission energies and the reorganization energies have been calculated for all the disubstituted derivatives and compared with mer-Alg3 and mer-AlND3.

2 Computational Details

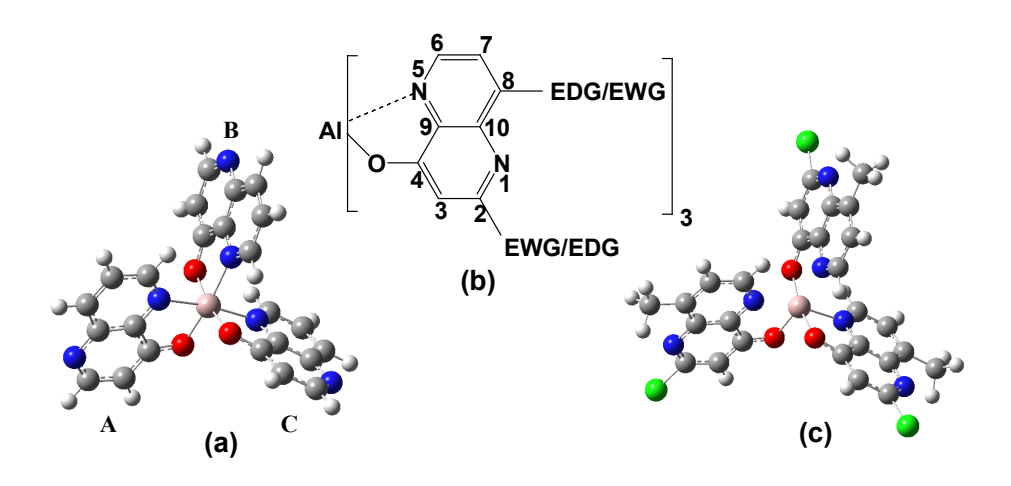
The ground state (S₀) geometries of all the disubstituted mer-AlND3-derivatives (1-8) in which the EDG and EWGs groups are substituted at positions 8 and 2 respectively

on ligands and vice versa (Fig 1). The geometry of these derivatives is constructed by using the reported x-ray coordinates of the parent mer-AlND3 [52], which possesses C,-symmetry. The geometry optimizations have been carried out using DFT/B3LYP/6-31G(D) method using G09 package [53]. This method has been proved to be a reliable approach for Alq3 and its derivatives [54-63], mer-AlND3 and its methyl derivatives [64]. During optimization the atomic positions of the all these derivatives have been fully relaxed without any constraints and only the lowestlying minima are reported. The optimizations have been carried using the Berny optimization algorithm with a default integration grid. The B3LYP functional consists of Becke's three-parameter hybrid exchange functional [65] combined with the Lee-Yang-Parr correlation functional [66]. Frequency calculations have been carried out to ensure that the optimized geometry has all positive frequencies and thus is a minimum on the potential energy surface. The first excited state (S₁) geometries have been optimized using the ab initio CIS approach [37] and previously this approach has been applied on mer-Alg3 and its derivatives [54-63], mer-AlND3 and its methyl derivatives [64] and other OLED materials [67-71] which has given reliable results. The absorption and emission spectra of these derivatives have been evaluated at by PBE0/6-31G(D) method using the B3LYP/6-31G(D) and CIS/6-31G(D) optimized geometries respectively. The reorganization energies which is one of the important parameters for determining the charge mobilities have been calculated at the B3LYP/6-31G(D) level for all these derivatives.

3 Results and discussion

3.1 Ground State geometries

The model disubstituted derivatives (1-8) used in this study are obtained by systematic substitution of EDG (-CH₂/NH₂) and EWG (-CN/Cl) at 8 and 2-positions respectively on each ligands of mer-AlND3 as shown in Fig.1, considering the reported parent mer-AlND3 crystal geometry [52]. The ligands are labeled with A-C designating the three naphthyridinato ligands substituted with different aryl EWG/EDGs in the 8 and 2-positions as shown in Fig.1. In these derivatives the central Al atom (+3 formal oxidation state) is surrounded by the three naphthyridinato ligands in a pseudo-octahedral configuration with the A- and C- naphthyridinato nitrogens and the B- and C- naphthyridinatooxygens trans to each other (Fig.1).



N*	Different ligands	Derivative	
8 CH ₃ , 2 Cl	tris(8-methyl-2-chloro-4-hydroxy-1,5-naphthyridinato) aluminum	1	
8 CH ₃ , 2 CN	tris(8-methyl-2-cyano-4-hydroxy-1,5-naphthyridinato) aluminum	2	
8 NH ₂ , 2 Cl	tris(8-amino-2-chloro-4-hydroxy-1,5-naphthyridinato) aluminum	3	
8 NH ₂ , 2 CN	tris(8-amino-2-cyano-4-hydroxy-1,5-naphthyridinato) aluminum	4	
8 Cl, 2 CH ₃	tris(8-chloro-2-methyl-4-hydroxy-1,5-naphthyridinato) aluminum	5	
8 CN, 2 CH ₃	tris(8-cyano-2-methyl-4-hydroxy-1,5-naphthyridinato) aluminum	6	
8 Cl, 2 NH ₂	tris(8-chloro-2-amino-4-hydroxy-1,5-naphthyridinato) aluminum	7	
8 CN, 2 NH ₂	tris(8-cyano-2-amino-4-hydroxy-1,5-naphthyridinato) aluminum	8	

*N = 8 or 2 denotes as positons at where "H"s of the ligand are substituted by EDG (- CH_3 or - NH_2) And EWG (-CI or -CN) – (b).

Figure 1: (a) The Geometry of *mer*-AIND3 with three ligands labeled as A-C (b) the atom numbering for the disubstituted *mer*-AIND3 complexes considered in this study (c) the structure of *mer*-tris(8-methyl-2-chloro-4-hydroxy-1,5-naphthyridinato) aluminumas an example.

The calculated geometrical parameters of (1-8) are shown in Table 1, along with the optimized parameters of mer-AlND3 and the experimental [52] parameters for the same are given for comparison. Variation in the calculated bond lengths and bond angles have been observed for all the disubstituted derivatives, when compared to calculated geometrical parameters of parent molecule (*mer*-AlND3). In type I disubstituted derivatives (1-4), the calculated bond lengths of Al-N_e and Al-O have been found to be shortened and lengthened respectively. The maximum decrease in Al-N₅ bond have been found to be 0.30 in both the complexes 3 and 4, and the minimum in 2 (0.008) and 1 (0.007) as compared to parent molecule. The maximum increase in the Al-O bond have been found to be 0.022 in 4 and 0.017 in 3 as compared to parent molecule, while negligible deviation has been found in 1 and 2. The shortening of Al-N_c bond follows the order: 4 = 3 > 2 > 1(Table 1). In type II disubstituted complexes (5-8) the Al-N₅ bond is lengthened i.e, 0.011 in 6 and 0.008 in 8 as compared to parent molecule, while negligible deviation has been found for 5 and 7. The calculated Al-O bond has

been shortened i.e., 0.007 in 6 and 0.006 in 8 as compared to parent molecule, while negligible deviation has been found for 5 and 7 (Table 1). By introducing the EDG at position 8 in the ligands, shortening of the Al-N_E bond has been observed in type I complexes. This may due to the increase in the electron density on N-atom of the pyridine ring. As a result the N₅-atom attracts Al towards itself leading to the decrease in the Al-N₅ bond length. Maximum Al-N_E bond length shortening have been observed in 3 and **4**, because in both the complexes strong EDG is present at position 8, which donates more electron towards N_eatom (vide supra) (Table 1). By introducing strong EWG at position 8 in the ligands, the Al-N_c bond length increases because it attract the electrons of N_s -atom towards itself there by a decrease in the electron density on N_s -atom resulting in an increase of the Al-N₅ bond length in 6 and 8. In the case of 5, the weakly deactivating group i.e., -Cl at position 8 and weakly acting group i.e., -CH, at position 2, balance the effect of each other, hence negligible change in the bond lengths. The Al-N_c bond in the complex is slightly shortened due the presence of the weakly deactivating

Table 1: Calculated bond lengths (in Å) and bond angles (in deg) of (1-8) in their ground state (S_o) computed at B3LYP/6-31G(D) level.

	Expª	mer-AlND3	1	2	3	4	5	6	7	8
Al-N _A	2.021	2.080	2.074	2.074	2.060	2.065	2.079	2.085	2.078	2.083
$Al-N_B$	2.050	2.111	2.104	2.103	2.081	2.081	2.111	2.122	2.106	2.115
$Al-N_c$	2.003	2.062	2.056	2.056	2.044	2.043	2.060	2.065	2.059	2.065
Al-O _A	1.861	1.866	1.869	1.869	1.883	1.888	1.864	1.861	1.866	1.864
Al-O _B	1.873	1.892	1.895	1.894	1.909	1.909	1.889	1.885	1.889	1.886
Al-O _c	1.869	1.893	1.896	1.895	1.909	1.908	1.891	1.888	1.892	1.888
N _A -Al-Nc	174.2	171.7	171.3	171.0	171.3	171.1	171.5	171.4	171.5	171.4
N_B -Al- O_A	172.9	173.0	172.8	172.7	172.6	172.6	172.6	172.9	172.5	172.7
O _C -Al-O _B	171.1	167.9	168.0	168.0	168.7	168.7	167.5	167.3	167.9	167.8
μ		3.728	5.722	7.503	6.995	8.956	2.096	0.455	0.848	2.781

^a Experimental data for mer-AlND3 from [52]

group (-Cl) at position 8 and the strong activating group (-NH₂) is at position 2, which in turn results in the less withdrawing effect than the donating effect (Table 1). It can be seen from the Table 1, the calculated bond angles for these disubstituted derivatives are in good agreement with bond angles of parent molecule. It can be seen from these results that the standard deviation values of the crystallographically derived bond lengths and bond angles range from 0.018-0.029 and 0.0797-0.0799 respectively depending on the substations. The ground state dipole moment (µ) values for 1-8 are computed at the B3LYP/6-31G(D) level are given in Table 1. Earlier studies have shown that the EDG/EWG has pronounced effect on the dipole moment of the substituted complex [58]. Here also it has been observed that the EDG/EWG affects the dipole moment of the studied derivatives (1-8). By substitution EDG at position 8 and EWG at position 2 (Type I) leads to μ > 6 and by reverting the substitution i.e., EDG at position 2 and EWG at position 8 (Type II) leads to μ < 3. The trend in the dipole moment in these disubstituted derivatives is as follows: 4 > 2 > 3 > 1 > mer-AlND3 > 8 > 5 > 7 > 6 (Table 1).

3.1.1 Structure and Energy of ground state frontier molecular orbitals

Since the frontier molecular orbitals i.e., HOMO and LUMOs play an important role in determining the excitation as well, charge transport properties have been computed for **1-8** using B3LYP/6-31G(D) method. It has been already reported that the HOMOs are localized mostly on A-ligand while LUMOs are localized on B-ligand in mer-AlND3 and its methyl derivatives [64]. The distribution patterns of

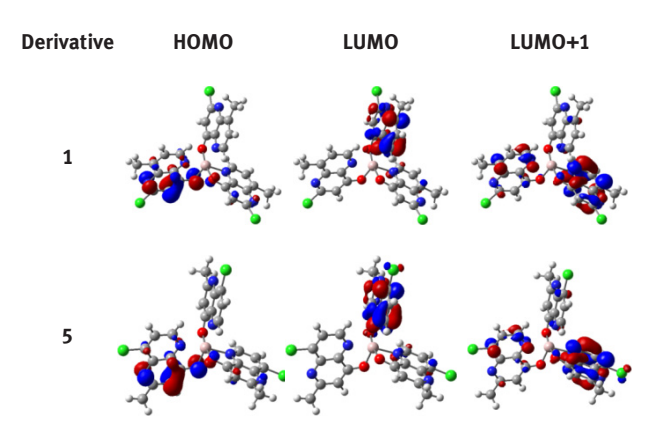


Figure 2: Frontier molecular orbitals (FMOs) for the ground states (S_o) of disubstituted derivatives of mer-AlND3 (1(type I) and 5 (type II)) computed at B3LYP/6-31G(D) method.

the HOMO, LUMO and LUMO+1 of all these disubstituted derivatives in their ground states are shown in Fig. 2 [1 (type I) and 5 (type II)] and Fig. S1 [supporting information for the distribution pattern of HOMOs and LUMOs+1 for (1-8)], which suggests the localization of frontier molecular orbitals. The HOMOs and LUMOs in these disubstituted derivatives show the similar trend of localization on A and B ligands, respectively as compared to mer-AlND3. It can be seen that HOMOs are located on the phenoxide oxygen and the N1, C2, C3 and C4 of the A-ligand, while LUMOs are located on the pyridyl ring of B-ligand. The LUMO+1 is mostly localized on C-ligand and on the N, C1, and C3 (pyridyl ring) of A-ligand (Figs. 2 and S1). The gap energies (E_n) have been calculated between the difference of HOMO and LUMO+1 energies because the major assignments for the absorptions are mainly from

Table 2: Calculated HOMO, LUMO, LUMO+1, and gap energies (E_{H.1} and E_) of (1-8) (in eVs) in their ground state (S_)computed at TD-PBEO/6-31G(D)//B3LYP/6-31G(D) level.

Derivative	номо	LUMO	LUMO+1	E _{H-L}	E _g
1	-6.544	-2.270	-2.033	4.274	4.511
2	-6.887	-2.785	-2.564	4.102	4.323
3	-6.044	-1.523	-1.318	4.521	4.726
4	-6.360	-2.101	-1.919	4.259	4.441
5	-6.346	-2.268	-2.039	4.078	4.307
6	-6.789	-3.140	-2.917	3.649	3.872
7	-6.126	-1.906	-1.697	4.220	4.429
8	-6.538	-2.743	-2.533	3.795	4.005
mer-AlND3	-6.188	-2.085	-1.843	4.103	4.345

 $E_{H-1} = |HOMO - LUMO|$; $E_g = |HOMO - (LUMO+1)|$

Table 3: The differences of the bond lengths (A°) between the first excited state (CIS/6-31G(D) and the ground state [HF/6-31G(D)] for ligands A ($\Delta A_{_{F,G}}$), B ($\Delta B_{_{F,G}}$) and C($\Delta C_{_{E,G}}$) respectively for 1 and 5 (for ligand bond labels see Fig. S3)

		1			5	
Ligand bond label	(ΔA _{E-G})	(ΔB _{E-G})	(ΔC _{E-G})	(ΔΑ _{E-G})	(ΔB _{E-G})	(ΔC _{E-G})
a (Al-O)	0.059	0.005	-0.002	0.067	0.005	-0.003
b (Al-N)	-0.068	-0.010	0.010	-0.070	-0.013	0.010
c	-0.025	0.000	-0.001	-0.016	0.001	-0.001
d	-0.005	0.000	-0.001	-0.007	0.001	-0.001
е	0.040	0.000	0.000	0.030	0.001	0.000
f	-0.023	0.000	-0.083	-0.028	0.001	0.000
g	0.054	0.000	0.083	0.060	0.000	0.000
h	-0.048	0.000	0.000	-0.054	0.000	0.000
i	-0.005	0.000	0.000	-0.005	0.000	0.000
j	0.045	0.000	0.000	0.047	0.000	0.000
k	-0.042	-0.001	0.000	-0.041	-0.001	0.000
ι	0.077	0.000	0.000	0.071	0.000	0.000
m	-0.006	0.001	0.000	-0.028	0.000	0.000
n	0.032	0.001	0.000	0.060	0.000	0.000

E - stands for excited-state and G - stands for the ground state

HOMO to LUMO+1. The HOMO, LUMO and LUMO+1 energy level of these disubstituted derivatives (except 3 and 7) are lower than AlND3 (Table 2). Among the type I complexes, it can be seen that the trend in all the HOMO, LUMO and LUMO+1 energies is as follows: 3 > 4 > 1 > 2, while the E follows: 3 > 1 > 4 > 2. In case of type II complexes, a general trend is observed in all the HOMO, LUMO and LUMO+1 and the E_g i.e., all these energies decrease in the same sequence 7 > 5 > 8 > 6 (Table 2). In all these derivatives (1-8), the E_g are found to be ~0.08–0.38 eV higher in 1,3,4 and 7 and ~ 0.22-0.47 eV lower in 2, 5, 6 and 8, when compared to mer-AlND3 (ca. 4.345 eV), while it is found to be ~0.02-0.65 eV higher than *mer*-Alg3 (ca. 3.856 eV) depending on the ligand substitutions (Table 2).

3.2 First Excited-state geometries

The experimental measurement on transition metal (Mg3) chelates solutions show a relatively large shift between the optical absorption and emission spectra [72]. This may be due to the significant geometrical differences between the ground and excited states. In the present work, studies have been carried out to investigate the geometrical changes associated with electronic excitations to the first singlet excited state (S₁). To attempt this, the CIS method has been used to determine the excited-state (S₁) geometry and this was compared with the HF optimized ground state geometry. The S₁ geometry optimizations for (1-8), have been carried out by CIS/6-31G(D) method using the corresponding HF/6-31G(D) optimized ground state (HF-S_o) geometries. In our previous study, the same approach has been adopted for mer-AlND3 and its methyl derivatives [64] and in earlier reports this method has been successfully applied on Alg3 and its derivatives [27,54-63]. The optimized bond lengths of the ground state at the optimized at HF/6-31G(D) (HF-S_o) and the excited state at the CIS/6-31G(D) (S₁)methods respectively along with the differences between the bond lengths of the S₁ and HF-S₀ states for ligands $A(\Delta A_{E-G})$, $B(\Delta B_{E-G})$ and $C(\Delta C_{EC})$ are shown in Table 3 [1 (type I) and 5 (type II)] and Table S1(a-d) [supportinginformation for (1-8)]. The scheme of the ligand bond labels used in Table 3, are shown in the supporting information (Fig. S3). It can be seen from the Table 3, that the positive and negative values in the difference columns indicate the bond elongation and contraction upon ground to S₁ transition respectively. The comparison of the (HF-S₀) and S₁ geometries for A-, B- and C-ligands in (1-8) indicates that the structural shift is predominantly localized on the ligand A. The Band C- ligands are slightly affected except for changes in the Al-O and Al-N bond lengths [Table 3 and Table S1(a-d)]. The changes of the bond lengths between the (HF-S_o) and S₁ states are in agreement with previous investigation [27,31,37,56,70]. To complement this study, the electron population changes associated to the transition have also been investigated, through a NBO (natural bond orbital) calculation [73]. The electronic charge distribution in HF-S₀ and S₁ states calculated with the HF/6-31G(D) and

Figure 3: The ligand atom labels used in the text for the disubstituted AlND3 complexes considered in this study in Table 4 and Table S2(a-d) (for EDG and EWG labels are not shown).

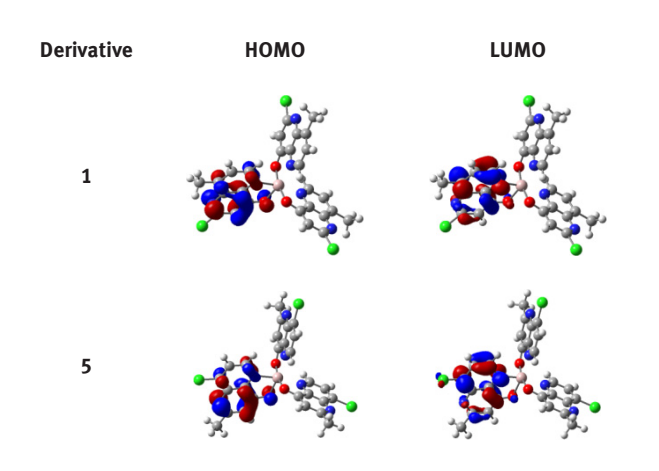


Figure 4: Frontier molecular orbitals (FMOs) for the excited states (S,) of disubstituted derivatives of mer-AlND3 (1(type I) and 5 (type II)) computed at CIS/31G (D) method.

CIS/31G (D) methods (respectively) are shown in Table 4 [1 (type I) and 5 (type II)] and Table S2(a-d) [supporting information for (1-8)] along with the relative differences in NBO charge for selected atoms in the two states i.e., HF-S_o and S, states. The ligand atom labels for the disubstituted AlND3 complexes are shown in Fig 3.It can be seen from Table 4 that the larger differences of the electron population's charges of the two states are mainly found in A-ligand, while those of the B- and C-ligands are negligibly small. This clearly indicates that the structural distortions in the disubstituted derivatives (1-8) are caused in the A-ligand. These results are in agreement with previous investigation [27,31,37,56,70]. Thus, the transition from the ground to the S, state yields significant structural changes in only one ligand while the other two ligands remain nearly the same. Hence the predominant relaxation of ligand A in the S₁ state may contribute to the observed difference between the optical properties.

3.2.1 Structure and Energy of excited state frontier molecular orbitals

The HOMO and LUMO distribution patterns of (1-8) in their excited states are shown in Fig. 4 [1 (type I) and 5 (type II)] and Fig. S4 [supporting information for the distribution pattern of HOMOs and LUMOs + 1 for (1-8)], which suggests the localization of frontier molecular orbitals. The HOMO is localized mainly on the pyridine-4-ol ring of A-ligand while the LUMO is localized mainly on the pyridyl ring of A-ligand (Figs. 3 and S4). The HOMO and LUMO energies of (1-8) computed using the TD-PBE0/6-31G(D)//CIS/6-31G(D) method are shown in Table 5. The gap energies (E,,) have been calculated between the difference of HOMO and LUMO energies because the major assignments for the emission are mainly from HOMO to LUMO (Table 5). Here also it can be seen that the HOMO and LUMO energy levels of all the complexes (except 3 and 7) are lower than that of both the AlND3 and Alq3. In the type I complexes both the HOMO and LUMO energies decrease in the same sequence i.e., 2 > 1 > 4 > 3, while the gap energies decrease in the sequence of 3 > 4 > 1 > 2. In type II complexes both the HOMO and LUMO energies decrease in the same sequence i.e., 6 > 8 > 5 > 7, while the gap energies decrease in the sequence of 7 > 5 > 8 > 6. Here also the gap energies in all these complexes (1-8) are found to be ~0.05-0.56 eV higher in 1, 3, 4, 5 and 7 and ~0.10-0.37 eV lower in 2, 6 and 8, when compared to mer-AlND3 (ca. 4.345 eV), while it is found to be ~0.27–1–1.19 eV higher than *mer*-Alq3 (ca. 3.224 eV) depending on the substitutions (Table 5).

3.3 Absorption and emission properties

In the earlier study [64] on mer-AlND3 and its methyl derivatives, the absorption and emission spectra have been calculated by using time dependent density functional theory (TDDFT) and we have shown that PBE0 gave reliable absorption and emission wave lengths among SVWN, BLYP, BP86, BPW91, B3LYP, B3P86, B3PW91, MPW1PW91 and PBE0 functionalities. We have also explained that the basis set has no significant effect on absorption wavelength and the absorption and emission energies have been calculated by TDDFT at the PBE0/6-31G(D) level using B3LYP/6-31G(D) and CIS/6-31G(D) optimized geometries respectively. Here also similar to the previous study the absorption and emission wavelengths of (1-8) have been computed at the same level of theory and are summarized in Table 6, along with the experimentally reported absorption and emission wavelengths of mer-AlND3 [52] for the sake of comparison. It can be seen in

Table 4: The NBO charges (Q) of the ligands in 1 and 5, in the optimized ground $(Q_{HF.SO})$ and first excited (Q_{SI}) states structures and the charge differences between $Q_{HF.SO}$ and Q_{SI} states calculated at the HF/6-31G(D) and CIS/6-31G(D) methods, respectively (for atom labels see Fig. S4) (for EDG and EWG labels are not shown).

	Deri	ivative-1								
		\mathbf{Q}_{HF-S0}			$\mathbf{Q}_{\mathrm{s}_{1}}$			$Q_{S1}-Q_{HF-SO}$)	
Atom		Α	В	С	Α	В	С	Α	В	c
0	1	-0.917	-0.917	-0.927	-0.882	-0.914	-0.928	0.035	0.002	-0.002
N	<u>2</u>	-0.631	-0.638	-0.642	-0.653	-0.646	-0.636	-0.022	-0.008	0.006
С	<u>3</u>	0.156	0.152	0.168	0.110	0.154	0.166	-0.046	0.002	-0.002
С	<u>4</u>	-0.308	-0.309	-0.307	-0.303	-0.310	-0.306	0.005	-0.001	0.001
С	<u>5</u>	0.086	0.083	0.084	0.100	0.086	0.083	0.014	0.003	-0.002
С	<u>6</u>	0.175	0.173	0.173	0.188	0.173	0.172	0.012	0.000	0.000
С	<u>Z</u>	0.318	0.315	0.315	0.290	0.315	0.315	-0.027	0.000	-0.001
С	<u>8</u>	-0.417	-0.418	-0.419	-0.419	-0.418	-0.419	-0.003	0.001	0.000
С	<u>9</u>	0.524	0.511	0.511	0.559	0.511	0.512	0.035	-0.001	0.001
С	<u>10</u>	0.108	0.098	0.107	0.111	0.100	0.107	0.003	0.001	0.000
N	<u>11</u>	-0.582	-0.578	-0.575	-0.612	-0.579	-0.575	-0.030	0.000	0.000
С		-0.653	-0.654	-0.653	-0.660	-0.654	-0.653	-0.007	0.000	0.000
Cl		-0.021	-0.016	-0.020	-0.003	-0.016	-0.021	0.018	0.001	0.000
Al		2.139			2.135			-0.004		
	Deri	ivative 5								
		\mathbf{Q}_{HF-S0}			$\mathbf{Q}_{\mathrm{s}_{1}}$			$Q_{S1} - Q_{HF-S}$	0	
Atom		Α	В	C	Α	В	C	Α	В	C
0	1	-0.925	-0.926	-0.936	-0.883	-0.924	-0.938	0.042	0.002	-0.002
N	<u>2</u>	-0.617	-0.624	-0.629	-0.639	-0.634	-0.621	-0.022	-0.010	0.007
С	<u>3</u>	0.140	0.136	0.153	0.093	0.139	0.151	-0.047	0.003	-0.002
С	<u>4</u>	-0.307	-0.308	-0.306	-0.298	-0.309	-0.306	0.009	-0.001	0.001
С	<u>5</u>	0.038	0.035	0.038	0.037	0.038	0.036	-0.001	0.003	-0.002
С	<u>6</u>	0.166	0.163	0.163	0.181	0.164	0.163	0.015	0.000	0.000
С	Z	0.346	0.346	0.344	0.330	0.346	0.344	-0.016	0.001	-0.001
С	<u>8</u>	-0.405	-0.405	-0.407	-0.410	-0.405	-0.406	-0.005	0.001	0.000
•	9	0.513	0.499	0.500	0.561	0.498	0.500	0.047	-0.001	0.001
				0.114	0.110	0.107	0.114	-0.006	0.002	0.000
С	<u>10</u>	0.115	0.105	0.114						
C C	<u>10</u> <u>11</u>	0.115 -0.580	0.105 -0.576	-0.574	-0.619	-0.576	-0.573	-0.039	0.000	0.001
C C N					-0.619 -0.657	-0.576 -0.662	-0.573 -0.661	-0.039 0.004	0.000	
C C N		-0.580	-0.576	-0.574						0.000
C C N C		-0.580 -0.661	-0.576 -0.662	-0.574 -0.661	-0.657	-0.662	-0.661	0.004	0.000	0.001 0.000 -0.001

all the disubstituted derivatives, the major transitions for absorption are from HOMO to LUMO+1 while for the emission are from HOMO to LUMO (Table 6). 1, 3 and 4 showed the blue shifts of absorption spectra ca 18 nm, 46 nm and 26 nm, while 6 and 8 showed red shifts of the absorption spectra ca 55 nm and 35 nm compared with the calculated *mer*-AlND3 values respectively. The λ_{abs} of 2, 5 and 7 are almost equal to mer-AlND3. The absorption spectra of 1, 3 and 4 are blue shifted due to the increase in the gap energies, where as 5, 6 and 8 are red shifted due to the decrease in the gap energies in their ground states. The λ_{abs} of **2,5** and **7** are comparable with *mer*-AlND3 due to the similar gap energies in their ground states

Table 5: Calculated HOMO, LUMO, and gap energies (E,,,) of (1-8)(in eVs) in their excited state (S,) computed at TD-PBE0/6-31G(D)//CIS/6-31G(D) level.

Derivative	номо	LUMO	E _{H-L}
1	-6.245	-2.164	4.081
2	-6.349	2.734	3.615
3	-5.788	-1.499	4.289
4	-6.073	-1.947	4.126
5	-6.045	-2.198	3.847
6	-6.492	-3.061	3.431
7	-5.826	-1.780	4.046
8	-6.298	-2.606	3.692
mer-AlND3	-5.894	-2.032	3.862

 $E_{H,I} = |HOMO-LUMO|$

(Table 6). The 1-4 and 7 showed blue shifts in emission spectra ca 34 nm, 18 nm, 69 nm, 60 nm and 33 nm, while 6 and 8 showed red shifts of the emission spectra ca 67 nm and 13 nm when compared with the calculated mer-AlND3 respectively. The $\lambda_{\mbox{\tiny emi}}$ of ${\bf 5}$ is almost equal to mer-AlND3, due to the similar gap energies in their excited states. The emission spectra of 1-4 and 7 are blue shifted due to increase in the gap energies while in 6 and **8** are red shifted due to the decrease in the gap energies in their excited states. Thus the derivatives namely 1-4 and 7 are good candidates for blue and the derivatives namely 6 and 8 are good candidates for red light emitting materials respectively, when compared to mer-AlND3. All the disubstituted complexes have showed hypsochromic shifts in both the absorption (except 6) and emission spectra when compared with the calculated absorption (ca 410 nm) and emission spectra (ca 523 nm) respectively of mer-Alq3. Thus these disubstituted derivatives can be used as good candidates for blue light emitting materials in OLEDs.

3.4 Charge transfer and Reorganization energies

Namely the band theory [74,75] and the hopping model [75-83] are widely used for describing the charge transport in organic materials. With the overlap of neighboring molecular orbitals the band is formed through which the conduction of the charge takes place according to the band theory model. On the other hand the hopping model

Table 6: Calculated absorption (λ_{nb}) and emission (λ_{em}) wavelengths (in nms) of (1-8) at TD-PBE0/6-31G(D) level.

Derivative	Major Transitions ^a	λ_{abs}	f⁵	Major Transitions	$\lambda_{_{emi}}$	f ^b
1	H → L+1(79%)	332	0.1478	H → L (72%)	368	0.1198
2	H → L+1(80%)	344	0.1654	H → L(80%)	384	0.1288
3	H → L+1(74%)	304	0.1516	H → L(80%)	333	0.2086
4	H → L+1(74%)	324	0.2022	H → L(79%)	342	0.2260
5	H → L+1(71%)	353	0.1296	H → L(77%)	399	0.1081
6	H → L+1(73%)	405	0.1062	H → L(71%)	469	0.0858
7	H → L+1(69%)	340	0.1095	H → L(78%)	369	0.1194
8	H → L+1(69%)	385	0.1012	H → L(70%)	415	0.1122
mer-AlND3	H → L+1(69%)	350 (341) ^c	0.1029	H → L(69%)	402 (433) ^c	0.0730

 $[^]a$ H, L and L+1 stands for HOMO, LUMO and LUMO + 1; b f is oscillator strength; c the experimental absorption (λ_{ab}) and emission wavelengths (λ_{emi}) of mer-AIND3 are taken from [52], which are shown in the parenthesis.

is more suitable where coupling between neighboring molecules are small, and this is more appropriate in our case here. Using this model the charge transport that is calculated here is the intermolecular process in which the charge hops between two molecules. The hole and electron transport process at the molecular level in the electroluminescent layer can then be portrayed as the electron transfer/hole transfer reactions between the neighboring molecules as [27,84-95]:

where M* is the neutral molecule interacting with neighboring oxidized or reduced M+/-. In the case of electron transport the interaction can be considered between a molecule in the neutral state interacting with a radical anion and in the case of hole transport the interaction can be considered between a molecule in the neutral state and cation. The rate constant for electron transfer $(k_{\rm el})$ can be defined using the Marcus theory as [84]:

$$K_{of} = (4\pi^2/h) \tau^2 (4\pi\lambda k_R T)^{-1/2} \exp(-\lambda/4k_R T)$$
 (1)

where τ is the transfer integral/coupling matrix element between neighboring molecules, h is the Plank's constant, λ is the reorganization energy, $k_{_{\rm B}}$ is the Boltzmann constant and T is the temperature. The two major parameters that determine transfer rates and ultimately the charge mobility are t and λ which should be maximum and minimum respectively for achieving significant charge transport. An evaluation of τ would require the relative positions of the molecules in the solid state as it is related to the energetic splitting of the frontier orbitals of the interacting molecules. To calculate the charge transfer integrals, the crystal data is required which is not available; so we have calculated one of the important parameters of mobility, i.e., reorganization energy for all these derivatives. The $\boldsymbol{\lambda}_{hole}$ and $\boldsymbol{\lambda}_{ele}$ can be used to estimate approximately the charge transport and balance between the holes and electrons. The reorganization energy for both the hole (λ_{hole}) and electron (λ_{ele}) transport are evaluated using the following formulas [64,90-92].

$$\lambda_{\text{hole}} = (\mathbf{M}_{+}^{*} - \mathbf{M}_{+}) + (\mathbf{M}_{\text{extion}}^{*} - \mathbf{M})$$
 (2)

$$\lambda_{ele} = (M_{-}^{*} - M_{-}) + (M_{anion}^{*} - M)$$
 (3)

where M is the optimized ground state energy of the neutral molecule, M₁(M₁) is the optimized energy of the cationic(anionic) molecule, $M^*_{cation}(M^*_{anion})$ is the energy of

the neutral molecule in cationic(anionic) geometry, and M *(M *) is the energy of the cationic (anionic) molecule in neutral geometry. In these calculations only the structural modification of the molecules are considered neglecting the polarization effect in the surrounding medium. The electron/hole transport is predictable from the electron (λ_{pole}) /hole (λ_{hole}) reorganization energies and in general has good agreement with the experimental observations [27,71,82,85-95].

Previously the reorganization energies for hole/ electron of mer-Alg3 and its derivatives [56,57,59,61,63] and mer-AlND3 [64] has been calculated at B3LYP/6-31G(D) level. Hence the reorganization energy calculations have been carried out for (1-8) using the same methodology and compared with AlND3 (Table 7). In general introduction of EDGs favor the p-channel materials while the introduction of EWDs promote the n-channels materials [96]. To calculate the mobility, the reorganization energy and transfer integrals are important parameters to calculate the mobility. In order to evaluate the transfer integral the crystal data is required which is not available, so we have calculated only one of the important parameter of mobility, i.e., reorganization energy. On the basis of reorganization energy, the hole and electron mobilities of **1, 2, 5** and **6** derivatives are comparable with *mer*-AlND3. From Table 7, it can be seen that the introduction of strongly activating -NH, group at position 8 (3 and 4) or position 2 (7 and 8) boost the electron reorganization energies in the disubstituted derivates compared with AlND3. The hole reorganization energies of 3,4 and 8 (except 7) are lower compared to the parent AlND3 By introducing weakly activating -CH3 group on position 8 (1 and 2) or position 2 (5 and 6) along with EWDs -Cl/-CN, the hole as well as electron reorganization energies are almost same as parent molecule (mer-AlND3). Introduction of weakly deactivating group -Cl does not affect the strength of reorganization energies for 1 and 5. This may be due to that the weakly deactivating group -Cl and weakly activating group -CH, counter balance the effect of each other. The electron reorganization energies of 2 and 6 are smaller than *mer*-AlND3. This may be due to the presence of strongly deactivating group -CN. It can be seen that the hole/electron reorganization energies of some of the disubstituted derivatives i.e., 1, 2, 5 and 6 are comparable with the mer-Alg3[89] and hence these derivatives might be good candidates for emitting materials possessing comparable charge carrier mobility as mer-Alg3. From these results, it is seen that the donor/acceptor substitution has a significant effect on the intrinsic charge mobilities on the disubstituted derivatives when compared to mer-

Table 7: Calculated reorganization energies (in eV) of (1-8) for hole (λ_{holo}) and electron (λ_{alo}) at B3LYP/6-31G(D) level.

	mer-AlND3	1	2	3	4	5	6	7	8
λ_{hole}	0.213	0.253	0.232	0.199	0.176	0.231	0.231	0.252	0.174
$\lambda_{_{ele}}$	0.236	0.279	0.207	0.512	0.321	0.269	0.224	0.341	0.309

Alg3. Thus these derivatives might be good candidates for emitting materials possessing comparable charge carrier mobility as mer-Alq3.

Acknowledgements: The authors thank the Director, IICT and the Head, Inorganic Chemistry division, IICT for their constant encouragement in this work.

4 Conclusions

We have designed some disubstituted derivatives of mer-AlND3 for OLEDs by introducing strong electron with drawing groups on position 8 and electron donating groups on position 2 on 4-hydroxy-1,5-naphthyridinato ligands and vice versa. The ground state structures of these disubstituted derivatives of mer-AlND3 have been optimized at the DFT/B3LYP/6-31G(D) level of theory. From the frontier molecular orbitals analysis it is seen that in these derivatives the HOMOs and LUMOs are localized mainly on the A-ligand and B-ligand respectively, similar to both the mer-AlND3 and Alq3. The CIS/6-31G(D) method has been used to obtain the S₁ states. The correlations between the structural relaxations in the excited state have been made for all these derivates and are found to be mainly localized on the different ligands. The absorption and emission spectra calculations are carried out using TD-PBE0/6-31G(D) method and are found to be comparable with both the mer-AlND3 and mer-Alq3. From the results it can be seen that the derivatives namely 1-4 and 7 are good candidates for blue and the derivatives namely 6 and 8 are good candidates for red light emitting materials respectively when compared to mer-AlND3. the disubstituted complexes have hypsochromic shifts in both the absorption and emission spectra when compared to Alq3. Thus these disubstituted derivatives can be used as good candidates for blue light emitting materials in OLEDS. The reorganization energies have been calculated at B3LYP/6-31G(D) level. From these results it can be seen that the hole/electron reorganization energies of some of the disubstituted derivatives i.e., 1, 2, 5 and 6 are comparable with the mer-Alq3 and hence these derivatives might be good candidates for emitting materials possessing comparable charge carrier mobility as mer-Alq3. Thus the theoretical study of structural, electronic and charge transport properties of such complexes may be useful in designing the efficient emitters useful in OLEDs.

References

- Sheats J.R., Antoniadis H., Hueschen M., Leonard W., Miller J., Moon R., et al., Organic Electroluminescent device, Science, 1996, 273, 884-888.
- Miyata S., Nalwa S., Organic Electroluminescent Materials and Devices, Gordon and Breach: Amsterdam, The Netherlands,
- [3] Friend R.H., Gymer R.W., Holmes A.B., Burroughes J.H., Marks R.N., Taliani C., et al., Electroluminescence in conjugated polymers, Nature, 1999, 397, 121-128.
- Kelly S.M., In: Connor J.A., (Ed.) Flat Panel Displays, Advanced Organic Materials Series, The Royal Society of Chemistry, Cambridge, 2000.
- [5] Mitsche U., Bauerle P. J., The electroluminescence of organic materials, Mater. Chem., 2000, 10, 1471-1507.
- Shinar J., Organic Light-Emitting Devices-A Survey, Springer, Berlin, 2003.
- Holmes A.B., Polymers Light the Way, Nature, 2003, 421, 800-
- [8] Chen C.H., Shi J., Metal chelates as emitting materials for organic electroluminescence, Coord. Chem. Rev., 1998, 171,161-
- Baldo M. A., Lamansky S., Burrows P. E., Thompson M.E., Forrest S.R. Very high- efficiency green organic light-emitting devices based on electrophosphorescence, Appl. Phys. Lett., 1999, 75, 4-6.
- [10] Adachi C., Baldo M. A., Thompson M.E., Forrest S.R., Nearly 100% internal phosphorescence efficiency in an organic lightemitting device, J. Appl. Phys., 2001, 90, 5048-5051.
- [11] Baldo M. A., O'Brien D. F., You Y., Shoustikov A., Sibley S., et al., Highly efficient phos- phorescent emission from organic electroluminescent devices, Nature., 1998, 395, 151 -154.
- [12] Cleave V, Yahioglu G., Barny P. L., Friend R. H., Tessler N., Harvesting Singlet and Triplet Energy in Polymer LEDs, Adv. Mater., 1999, 11, 285-288.
- [13] Sajoto T., Djurovich P. I., Tamayo A., Yousufuddin M., Bau R., Thompson M. E., Holmes R. J., Forrest S. R., Blue and Near-UV Phosphorescence from Iridium Complexes with Cyclometalated Pyrazolyl or N-Heterocyclic Carbene Ligands, Inorg. Chem., 2005, 44, 7992-8003.
- [14] Makedonas C., Mitsopoulou. C. A., Tuning the properties of M(diimine)(dithiolate) complexes - The role of the metal and solvent effect. A combined experimental, DFT and TDDFT study, Inorg. Chim. Acta., 2007, 360, 3997-4009.

- [15] Lacroix P. G., Averseng F., Malfant I., Nakatani K., Synthesis, crystal structures, and molecular hyperpolarizabilities of a new Schiff base ligand, and its copper(II), nickel(II), and cobalt(II) metal complexes, Inorg. Chim. Acta., 2004, 357, 3825-3835.
- [16] Yersin H., Donges D., Low-lying electronic states and photophysical properties of organo-metallic Pd(II) and Pt(II) compounds. Modern research trends presented in detailed case studies in: Transition Metal and Rare Earth Compounds. Excited States, Transitions and Interactions Vol II Springer-Verlag Berlin, (Ed.) Yersin H., Top. Curr. Chem., 2001, 214, 81-182.
- [17] Srivastava R., Joshi L. R., The effect of substituted 1,2,4-triazole moiety on the emission, phosphorescent properties of the blue emitting heteroleptic iridium(III) complexes and the OLED performance: a theoretical study Phys Chem. Chem. Phys., 2014,16, 17284-17294.
- [18] Srivastava R., Laxmikanthrao J., Bhanuprakash K., Theoretical study of electronic struc- tures and opto-electronic properties of iridium(III) complexes containing benzoxazole derivatives and different ancillary β-diketonate ligands Comput. Theor. Chem., 2014,1035, 51-59.
- [19] Hung L.S., Chen C. H., Recent progress of molecular organic electroluminescent materials and devices, Mater. Sci. Eng. Rev., 2002, 39, 143-222.
- [20] Holder E., Langeveld B. M.W., Schubert U.S., New Trends in the use of Transition Metal- Ligand complexes For Applications in Electroluminescent Devices, Adv. Mater., 2005, 17, 1109-1121.
- [21] Tang C.W., VanSlyke S.A., Organic electroluminescent diodes, Appl. Phys. Lett., 1987, 51, 913-915.
- [22] Tang C.W., VanSlyke S.A., Chen C.H., Electroluminescence of doped organic thin films J. Appl. Phys., 1989, 65, 3610-3613.
- [23] Hamada Y., The development of chelate metal complexes as an organic electroluminescent Material, IEEE Trans Electron Devices 1997, 44, 1208-1217.
- [24] VanSlyke S.A., Chen C.H., Tang C.W., Organic electroluminescent devices with improved stability, Appl. Phys. Lett., 1996, 69, 2160-2162.
- [25] Bacon A.D., Zerner M.C., An intermediate neglect of differential overlap theory for transition metal complexes: Fe, Co and Cu chlorides, Theor. Chim. Acta., 1979, 53, 21-54.
- [26] Burrows P.E., Shen Z., Bulovic V., Mc Carty D.M., Forrest S.R., Cronin J.A., Thompson M.E., Relationship between electroluminescence and current transport in organic heterojunction light-emitting devices, J. Appl. Phys., 1996, 79, 7991-
- [27] Curioni A., Boero M., Andreoni W., Alq3: ab initio calculations of its structural and electronic properties in neutral and charged states, Chem. Phys. Lett., 1998, 294, 263-271.
- [28] Curioni A., Andreoni W., Treusch R., Himpsel R.F., Haskal E., Seidler P., Kakar S, van Buuren T, Terminello L.J., Atom-resolved electronic spectra for Alq3 from theory and experiment J. Appl. Phys. Lett., 1998, 72, 1575-1577.
- [29] Halls M.D., Aroca R., Vibrational spectra and structure of tris (8-hydroxyquinoline) aluminum (III), Can. J. Chem., 1998, 76, 1730-1736.
- [30] Stampor W, Kalinowski J, Marconi G, Di Marco P, Fattori V, Giro G., Electroabsorption study of excited states in tris 8-hydroxyquinoline aluminum complex, Chem. Phys. Lett., 1998, 283, 373-380.

- [31] Curioni A., Andreoni W., Metal-Alq, Complexes: The Nature of the Chemical Bonding J. Am. Chem. Soc., 1999, 121, 8216-8220.
- [32] Johansson N., Osada T., Stafstrom S., Bredas J.L., Electronic structure of tris(8-hydroxy-quinoline) aluminum thin films in the pristine and reduced states, J. Chem. Phys., 1999, 111, 2157-2163.
- [33] Kushto, GP, lizumi Y, Kido J, Kafafi ZH., A Matrix-Isolation Spectroscopic and Theoretical Investigation of Tris(8hydroxyguinolinato)aluminum(III) and Tris(4-methyl-8hydroxyquinolinato) aluminum(III), J Phys. Chem. A, 2000, 104, 3670-3680.
- [34] Tung Y.L., Wu P.C., Liu C.S., Chi Y., Yu J.K., Hu Y.H., et al., Highly Efficient Red Phosphorescent Osmium(II) complexes for OLED Applications, Organometallics, 2004, 23, 3745-3748.
- [35] Anderson S., Weaver M.S., Hudson A.J., Materials for organic aluminium vs. boron, Synth. Met., electroluminescence: 2000, 111-112, 459-463.
- [36] Martin R.L., Kress J.D., Campbell I.H., Smith D.L., Molecular and solid-state properties of tris-(8-hydroxyquinolate)-aluminum Phys. Rev. B., 2000, 61,15804-15811.
- [37] Halls M.D., Schlegel, H.B., Molecular Orbital Study of the First Excited State of the OLED Material Tris (8-hydroxyquinoline) aluminum (III), Chem. Mater., 2001, 13, 2632-2640.
- [38] Sugimoto M., Sakaki S., Sakanoue K., Newton M.D., Theory of emission state of tris(8-quinolinolato)aluminum and its related compounds, J. Appl. Phys., 2001, 90,6092-6097.
- [39] Amati M., Lelj F., Are UV-Vis and luminescence spectra of Alq3 [aluminumtris(8- hydroxy quinolinate)] d-phase compatible with the presence of the fac-Alq3 isomer? A TD-DFT investigation, Chem. Phys Lett., 2002, 358,144-150.
- [40] Ballardini R, Varani G, Indelli M.T., Scandola F., Phosphorescent 8-quinolinol metal chelates. Excited-state properties and redox behavior, Inorg. Chem., 1986, 25, 3858-3865.
- [41] Vogler A, Kunkely H., 2001, In: Yersin, H (ed) Luminescent Metal Complexes: Diversity of Excited States, Topics in Current Chemistry Vol 213, Transition Metal and Rare Earth Compounds: Excited States, Transitions, Interactions Springer-Verlag: Berlin, 2001.
- [42] Shinar J., Organic Light-Emitting Devices A Survey, Springer, Berlin., 2003.
- [43] Yu J., Shen Z., Sakuratani Y., Suzuki H., Tokita M., Miyata S., A Novel Blue Light Emitting Diode Using Tris(2,3-methyl-8hydroxyquinoline) Aluminum(III) as Emitter, Jpn. J. Appl. Phys., 1999, 38, 6762-6763.
- [44] Sapochak L.S., Padmaperuma A., Washton N., Endrino F., Schmett G.T., Marshall J., Fogarty D., Burrows P.E., Forrest S.R., Effects of Systematic Methyl Substitution of Metal (III) Tris(n-Methyl-8-Quinolinolato) Chelates on Material Properties for Optimum Electro- luminescence Device Performance, J. Am. Chem. Soc., 2001, 123, 6300-6307.
- [45] Pohl R, Anzenbacher P. Jr., Emission Color Tuning in AlQ3 Complexes with Extended Conjugated Chromophores Org. Lett., 2004, 5, 2769-2772.
- [46] Pohl R, Montes V.A, Shinar J., Anzenbacher P. Jr., Red-Green-Blue Emission from Tris (5-aryl-8-quinolinolate)Al(III) Complexes, J. Org. Chem., 2004, 69,1723-1725.
- [47] Montes V.A., Li G., Pohl R., Shinar J., Anzenbacher P Jr., Effective Color Tuning in Organic Light-Emitting Diodes Based on Aluminum Tris(5-aryl-8-hydroxyquinoline) Complexes, Adv. Mater., 2004, 16, 2001-2003.

- [48] Perez-Bolivar C., Montes V.A, Anzenbacher P Jr., True Blue: Blue-Emitting Aluminum(III)Quinolinolate Complexes, Inorg Chem., 2004, 45, 9610-9612.
- [49] Jang H., Do L.M., Kim Y., Kim J.G., Zyung T., Do Y., Synthesis and luminescence behaviors of aluminum complex with mixed ligands, Synth. Met., 2001, 121, 1669-1670.
- [50] Hopkins T.A., Meerholz K., Shaheen S., Anderson M.L., Schmidt A., Kippelen B., Padias A.B., Hall H.K. Jr., Peyghambarian N., Armstrong N.R., Substituted Aluminum and Zinc Ouinolates with Blue-Shifted Absorbance/Luminescence Bands: Synthesis and Spectroscopic, Photoluminescence, and Electroluminescence Characterization, Chem. Mater., 1996, 8,344-351.
- [51] Shi Y.W., Shi M.M., Huang J.C., Chen H.Z., Wang M., Liu X.D., Ma Y.G., Xu H., Yang B., Fluorinated Alq, derivatives with tunable optical properties, Chem. Commun., 2006, 18,1941-1943.
- [52] Liao.S. H., Shiu J. R., Liu S.W., Yeh S. J., Chen Y. H., Chen C. T., Chow T. J., Wu C. I., Hydroxynaphthyridine-Derived Group III Metal Chelates: Wide Band Gap and Deep Blue Analogues of Green Alq, (Tris(8-hydroxyquinolate)aluminum) and Their Versatile Applications for Organic Light-Emitting Diodes J. Am. Chem. Soc., 2009, 131, 763-777.
- [53] Frisch M.J., Trucks G.W., Schlegel H.B., Scuseria G.E., et al., Gaussian 09, Revision A.02, Gaussian, Inc., Wallingford CT, 2009
- [54] Han Y.K., Lee S. U., Molecular orbital study on the ground and excited states of methyl substituted tris(8-hydroxyquinoline) aluminum(III), Chem. Phys. Lett., 2002, 366, 9-16.
- [55] Zhang J., Frenking G., Quantum chemical analysis of the chemical bonds in Mq3 (M = Al",Ga") as emitting material for OLED, Chem. Phys Lett., 2004, 394, 120-125.
- [56] Zhang J., Frenking G., Quantum Chemical Analysis of the Chemical Bonds in Tris(8- hydroxyquinolinato)aluminum as a Key Emitting Material for OLED, J Phys. Chem. A., 2004, 108, 10296-10301.
- [57] Gahungu G., Zhang J., CH/N Substituted mer-Gag3 and mer-Alg3 Derivatives: An Effective Approach for the Tuning of Emitting Color, J Phys. Chem. B 2005, 109, 17762-17767.
- [58] Wang W., Dong S., Yin S., Yang J., Lu J., Theoretical investigation on the structure and electronic properties of AlgaR (R = 8-hydroxyguinoline, OH, phenolate and phenyl phenollate) and its derivatives, J Mol Struct: Theochem., 2008, 867, 116-121.
- [59] Irfan A., Cui R., Zhang J., Explaining the HOMO and LUMO distribution on individual ligands in mer-Alq3 and its "CH"/N substituted derivatives J Mol Struct: Theochem., 2008, 850, 79-83.
- [60] Irfan A., Cui R, Zhang J., Fluorinated derivatives of mer-Alq3: energy decomposition analysis, optical properties, and charge transfer study, Theor. Chem. Acc., 2009, 122, 275-281.
- [61] Irfan A., Zhang J., Effect of one ligand substitution on charge transfer and optical properties in mer-Alq3:a theoretical study, Theor. Chem. Acc., 2009, 124, 339-344.
- [62] Fang X.H., Hao Y.Y., Han P.D., Xu B.S., Theoretical study on charge transport properties of a dinuclear aluminum 8-hydroxyquinoline complex J Mol Struct: Theochem., 2009, 896, 44-48.
- [63] Rao J.L., Bhanuprakash K., Structure and electronic properties of Alq3 derivatives with electron acceptor/donor groups at the C4 positions of the quinolate ligands: a theoretical study, J. Mol. Model., 2011, 17, 3039-3046.

- [64] Rao J.L., Bhanuprakash K., Structure and electronic properties of tris(4-hydroxy-1,5- naphthyridinato) aluminum (AIND3) and its methyl derivatives: a theoretical study, Theor. Chem. Acc., 2011, 129, 131-139.
- [65] Becke A. D., Density-functional thermochemistry. III. The role of exact exchange, J. Chem. Phys., 1993, 98, 5648-5652.
- [66] Lee C., Yang W., Parr R. G., Development of the Colle-Salvetti correlation-energy formula into a functional of the electron density, Phys. Rev., 1988, 37, 785-789.
- [67] Yang Z., Yang S., Zhang J., Ground- and Excited-State Proton Transfer and Rotamerism in 2-(2-Hydroxyphenyl)-5-phenyl-1,3,4-oxadiazole and Its O/NH or S-Substituted Derivatives, J. Phys. Chem. A, 2007, 111, 6354-6360.
- [68] Hu B., Gahungu G., Zhang J., Optical Properties of the Phosphorescent Trinuclear Copper(I) Complexes of Pyrazolates: Insights from Theory, J. Phys. Chem. A, 2007, 111, 4965-4973.
- [69] Sun M., Niu B., Zhang J., Computational study on optical and electronic properties of the CH/N substituted emitting materials based on spirosilabifluorene derivatives J. Mol. Struct: Theochem., 2008, 862,85-91.
- [70] Teng Y.L., Kan Y.H., Su Z.M., Liao Y., Yang S.Y., Wang R.S., Timedependent density functional theory study on electronic and spectroscopic properties for Ph2Bq and its complexes, Theor Chem. Acc., 2007, 117,1-5.
- [71] Brinkmann M, Gadret G, Muccini M, Taliani C, Masciocchi N, Sironi A., Correlation between Molecular Packing and Optical Properties in Different Crystalline Polymorphs and Amorphous Thin Films of mer-Tris(8-hydroxyquinoline)aluminum(III), J. Am. Chem. Soc., 2000, 122, 5147-5157.
- [72] Ghedini M., Deda M. L., Aiello I., Grisolia A., Synthesis and photophysical characterisa-tion of soluble photoluminescent metal complexes with substituted 8-Hydroxyquinolines Synth. Met., 2003, 138, 189-192.
- [73] Reed A. E., Curtiss L. A, Weinhold F., Intermolecular interactions from a natural bond orbital, donor-acceptor viewpoint, Chem. Rev.,1988, 88, 899-926.
- [74] Bredas J. L., Calbert J. P., da Silva Filho D. A., Cornil J., Organic semiconductors: A theoretical characterization of the basic parameters governing charge transport, Proc. Natl. Acad. Sci., 2002, 99, 5804-5809.
- [75] Cheng Y. C., Silbey R. J., da Silva Filho D. A., Calbert J. P., Cormil J., Bredas J. L., Three-dimensional band structure and bandlike mobility in oligoacene single crystals: A theoretical investigation, J. Chem. Phys., 2003, 118, 3764-3774.
- [76] Marcus R.A., Electron transfer reactions in chemistry. Theory and experiment, Rev. Mod. Phys., 1993, 65, 599-610.
- [77] Sakanoue K., Motoda M., Sugimoto M., Sakaki S., A Molecular Orbital Study on the Hole Transport Property of Organic Amine Compounds J. Phys. Chem. A, 1999, 103, 5551-5556.
- [78] Malagoli M., Bredas J. L., Density functional theory study of the geometric structure and energetics of triphenylaminebased hole-transporting molecules, Chem. Phys. Lett., 2000, 327, 13-17.
- [79] Li X. Y., Tong J., He F. C, Ab initio calculation for inner reorganization energy of gas- phase electron transfer in organic molecule-ion, Chem. Phys., 2000, 260, 283-294.
- [80] Nelsen S. F, Trieber II D. A., Ismagilov R. F., Teki Y., Solvent Effects on Charge Transfer Bands of Nitrogen-Centered

- Intervalence Compounds, J. Am. Chem. Soc., 2001, 123, 5684-
- [81] Nelsen S. F., Blomgren F., Estimation of Electron Transfer Parameters from AM1 Calculations, J., Org. Chem., 2001, 66, 6551-6559.
- [82] Lin B.C., Cheng C.P., Lao Z.P.M., Optical Properties of the Phosphorescent Trinuclear Copper(I) Complexes of Pyrazolates: Insights from Theory, J. Phys. Chem. A., 2003, 107, 5241-5251.
- [83] Barbara P., Meyer T., Ratner M., Contemporary Issues in Electron Transfer Research, J. Phys. Chem., 1996, 100, 13148-
- [84] Marcus R.A., On the Theory of Oxidation-Reduction Reactions Involving Electron Transfer. I, J. Chem. Phys., 1956, 24, 966-978.
- [85] Cornil J., Lemaur V., Calbert J.P., Bredas J.L., Charge Transport in Discotic Liquid Crystals: A Molecular Scale Description, Adv. Mater., 2002, 14, 726-729.
- [86] Wang I., Estelle B.A., Olivier S., Alain I., Baldeck P.L., Absorption and fluorescence properties of bifluorene crystal and microcrystals, J. Opt. A: Pure. Appl. Opt. 2002, 4, S258-
- [87] Deng W.Q., Goddard III W.A., Predictions of Hole Mobilities in Oligoacene Organic Semiconductors from Quantum Mechanical Calculations, J. Phys. Chem. B, 2004, 108, 8614-
- [88] Bredas J.L., Beljonne D., Coropceanu V., Cornil J., Charge-Transfer and Energy-Transfer Processes in π-Conjugated Oligomers and Polymers: A Molecular Picture, Chem. Rev, 2004, 104, 4971-5004.
- [89] Lin B.C., Cheng C.P., You Z.Q., Hsu C.P., Charge Transport Properties of Tris(8- hydroxyquinolinato)aluminum(III): Why It Is an Electron Transporter, J. Am. Chem. Soc., 2004, 127, 66-67.

- [90] Torrent M.M., Durkut M., Hadley P., Ribas X., Rovira C., High Mobility of Dithiophene- Tetrathiafulvalene Single-Crystal Organic Field Effect Transistors, J. Am. Chem. Soc., 2004, 126, 984-985.
- [91] Bromley S.T., Torrent M.M., Hadley P., Rovira C., Importance of Intermolecular Interactions in Assessing Hopping Mobilities in Organic Field Effect Transistors: Pentacene versus Dithiophene-tetrathiafulvalene, J. Am. Chem. Soc., 2004, 126, 6544- 6545.
- [92] Cornil J., Calbert J.P., Bredas J.L., Electronic Structure of the Pentacene Single Crystal: Relation to Transport Properties, J. Am. Chem. Soc., 2001, 123, 1250-1251.
- [93] Pan J.H., Chou Y.M., Chiu H.L., Wang B.C., Theoretical investigations of the molecular conformation and reorganization energies in the organic diamines as holetransporting materials, J. Phys. Org. Chem., 2007, 20, 743-753.
- [94] Yang L., Feng J.K., Ren A.M., Theoretical study on electronic structure and optical properties of novel donor-acceptor conjugated copolymers derived from benzothiadiazole and benzoselenadiazole, J Mol Struct: Theo. Chem., 2007, 816,
- [95] Liu Y.L., Feng J.K., Ren A.M., Theoretical study of optical and electronic properties of the bis-dipolar diphenylaminoendcapped oligoarylfluorenes as promising light emitting materials, J. Phys.Org. Chem., 2007, 20, 600-609.
- [96] Zaumseil J., Sirringhaus H., Electron and Ambipolar Transport in Organic Field-Effect Transistors, Chem. Rev., 2007, 107, 1296-1323.

Supplemental Material: The online version of this article (DOI: 10.1515/chem-2016-0001) offers supplementary material.